RSC Advances

Influence of Addition of Vapor Grown Carbon Fiber on Mechanical, Thermal and Biodegradation Properties of Lignin Nanoparticles Filled Bio-Poly (trimethylene terephthalate) Hybrid Nanocomposites

Journal:	*RSC Advances*
Manuscript ID:	RA-ART-04-2015-007828.R1
Article Type:	Paper
Date Submitted by the Author:	15-Jun-2015
Complete List of Authors:	Gupta, Arun; CIPET, LARPM Mohanty, Smita; Laboratory for Advanced Research in Polymeric Materials (LARPM), Central Institute of Plastics and Engineering and Technology (CIPET), Nayak, Sanjay K.; CIPET, LARPM

Influence of Addition of Vapor Grown Carbon Fiber on Mechanical, Thermal and Biodegradation Properties of Lignin Nanoparticles Filled Bio-Poly (trimethylene terephthalate) Hybrid Nanocomposites

ARUN KUMAR GUPTA, SMITA MOHANTY*, S. K. NAYAK

Laboratory for Advanced Research in Polymeric Materials (LARPM), Central Institute Of Plastics Engineering and Technology (CIPET) Bhubaneswar, Orissa 751024, India

***Corresponding Author, E-mail: papers.journal@gmail.com**

T: +91-674-2742852. F: +91-674-2743863

ABSTRACT

Bio-Poly (trimethylene terephthalate) (Bio-PTT) hybrid nanocomposites constituting of 1.5 wt.% of lignin nanoparticles (LNP) and variable wt.% of vapor-grown carbon fibers (VGCF) were prepared using melt extrusion followed by microinjection molding technique. Mechanical results revealed an improvement in tensile flexural and impact properties of bio-PTT with 1.5 wt. % LNP and bio-PTT hybrid naonocomposites with the incorporation of 7 wt. % of VGCF, respectively. The thermal properties of the hybrid nanocomposites have been investigated using HDT, and TGA. FTIR analysis confirmed the formation of hydrogen bond between aliphatic –OH groups of LNP with carbonyl group of bio-PTT matrix. The water resistance of bio-PTT/LNP/VGCF hybrid nanocomposites was higher than that of bio-PTT/LNP nanocomposites as well as bio-PTT matrix. In addition, the morphological changes in hybrid nanocomposites were also monitored through scanninig electron microscopy (SEM).

Keywords: Hybrid Nanocomposites, Vapor Grown Carbon Fibers, Lignin Nanoparticles, Biodegradability behavior, TEM, FTIR

1. Introduction

Research in the area of nanocomposites have received considerable interests in the recent years, owing to their properties their manifold applications ranging from automotive to electronics, medical, packaging etc. Currently, with the growing demand of renewable resource based polymers more attention is being paid in the development of bio-based or biodegradable polymers to reduce the carbon footprints on the environment while reducing the dependency of the petroleum based feedstock.[1,2]

Bio-based nanocomposites are the materials which are primarily made from renewable nanoparticles (e.g., cellulose whiskers, microfibril cellulose, and natural fibers) and petroleum-derived polymers like polypropylene (PP), polyethylene (PE), and epoxies. Conversely, biodegradable nanocomposites are derived from biopolymers (e.g., polylactic acid (PLA), polyhydroxyalkanoates (PHA), polyhydroxybutyrate (PHB) and poly(butylene adipate-co-terephthalate) PBAT) and nanofilers (e.g., carbon nanotubes and nanoclay) which also comes under green nanocomposites.[3,4] The materials have huge potential over their synthetic counterparts for widespread applications. The hybrid green nanocomposites can be produced from combination of two fillers reinforced within a biopolymer.[5] The synergism of two different fillers results in improvement in the properties which balancing its processibility as well as biodegradability.[6,7]

As a base matrix poly (trimethylene terephthalate) (PTT) has been extensively studied[8-11]. PTT gives many beneficial properties with good tensile behavior, outstanding elastic recovery and thermal stability, making it an ideal candidate for use in applications such as automotive component or engineering plastic. Moreover, PTT an aromatic polyester is prepared by the polycondensation reaction between propane-1,3-diol and terephthalic acid or dimethyl

terephthalate, has gained commercialization over the last years.[12] The polymers and materials derived from mixed renewable and fossil fuel sources not only show strong promise in alleviating the fossil fuel dependency but also have an added advantage of delivering the desired performance from a more sustainable stock material.[13] Bio-PTT in which the 1, 3 propanediol has been sourced from corn starch can be potentially in various value added applicants.

The use of LNP as nanofiller for the development of hybrid nanocomposites is a new area of interest because of its low cost, low density, renewable, low energy consumption, high specific properties, modest abrasivity during processing, biodegradability, reactive surface etc.[14] Lignin is an aromatic polymer with a complex structure; the abundance and relatively low price of this renewable resource are good reasons for searching for the obtaining of micro- and nanoparticles. In an attempt to identify reinforcing capability of LNP suitable for the production of nanocomposites wherein physico-chemical, mechanical, thermal properties and other desired attributes can be controlled and tailored, we investigated the potential of lignin nanoparticle as a reinforcing agent in bio-PTT matrix.[14-16]

Similarly, VGCF have attracted great deal of interest in many engineering applications for their high tensile strength and high aspect ratio. There are many studies[17-20] on the mechanical properties of polymer composites filled with VGCF. Due to their excellent mechanical, electrical and thermal properties, VGCF has been used as hybrid reinforcement agent for polymer in order to improve the strength, rigidity and thermal properties of polymer matrix.[21]

In this study, bio-PTT hybrid nanocomposite reinforced with optimal quantity of by LNP and VGCF have been fabricated through melt extrusion followed by microinjection moulding. These nanocompositess were subjected to mechanical, thermal, water absorption,

biodegradation, and morphological properties for evaluating its viability for suitable end-use application.

2. Experimental

2.1 Materials

Poly (trimethylene terephthalate) (PTT) of injection grade Biomax$^{(R)}$ PTT-1002 with 37% by weight bio-sourced, intrinsic viscosity (IV) of 1.02 dl/g, melt flow index (MFI) of 19.3 g/10 min, and density of 1.3 g/cc was supplied by M/s Dupont Packaging and industrial Polymer Ltd Mumbai, India. Lignin (Lignin protobind-1000) with density of 0.55 g/cc and micronsize of >500 μm was obtained from M/s Greencone Environs Pvt. Ltd, Hoshiarpur Punjab, India. Vapor grown carbon fiber (VGCF) was supplied by M/s Sigma-Aldrich, India with fiber diameter 150 nm and length of 10-20 μm and density of 2.0 g/cc, specific surface area of 13 m^2/g. All other solvents and chemicals of AR grade were purchased from M/s Mohaptara Scientific Odisha, India. Comparison of bio-PTT properties with other grade of PTT supplied by DuPont is depicted in Table 1.

Table 1. Typical properties of Bio-PTT and PTT

2.2 Methods

2.2.2 Synthesis of Lignin nanoparticles (LNP)

The lignin particle were initially cleaned with distilled water, dried and weighed. Subsequently, they were sieved in a sieve analyzer and the particles below 100 μm were collected for preparation of LNP. 1.4 gm lignin (below 100 μm) was dissolved in 250 ml ethylene glycol to prepare 2.8 wt. % lignin solutions, under stirring for 6 h at room temperature. Prior to precipitation the solution was filtered through a 0.4 mm micro filter to remove the insoluble impurities from lignin. Hydrochloric acid (8.00 cm^3, 0.025M) was added to 90 ml of

the filtered lignin solution at a rate of 0.5 ml/min. The solution was then dialysed in a 5 L beaker for three days changing the water three times daily. The resulting product was recovered by precipitation at pH 2 with 1N HCl solution, and then separated by centrifugation. The solid phase was washed twice with distilled water and subsequently dried and weighed. The resulting product was subjected to particle size analysis.

2.2.1 Preparation of LNP and VGCF reinforced bio-PTT hybrid green nanocomposites

Initially in the first step, bio-PTT/ LNP nanocomposites were prepared at an optimized composition of 1.5 wt% LNP loading, on the basis of mechanical studies. The compounding was carried out using a melt mixer (Haake Rheocord 9000, M/s Haake, Germany) having two banbury rotors and a mixing chamber of 69 cm^3 volumetric capacity at a processes temperature of 235 ^{0}C – 245 ^{0}C for 10 minutes. The same process in the second step, bio-PTT/LNP/VGCF hybrid nanocomposites containing different weight percentage of VGCF i.e. 3, 5, 7 and 10 wt % were prepared at a temperature of 245 ºC, with mixing speed of 45 rpm for a duration of 10 min using the same melt mixer Haake Rheocord. All compounded mixers were collected and stored in zipped bags before use. For sample preparation, each composition was cut in small pieces using a mechanical cutting device and subjected to melt extrusion followed by injection moulding (Microcompounder with injection jet, X-Plore, DSM-Netherlands micro 15 ml) at 245 ^{0}C with screw speed of 45 rpm and for duration of 15 min. Subsequently the melt mixes were injection molded at 35 ^{0}C and pressure 90 bars. Prior to preparation, the bio-PTT pellets, LNP and VGCF were pre-dried at 110 ^{0}C for 24 hours, 70 ^{0}C for 2 hours and 120 ^{0}C for 6 hours, respectively in vacuum oven.

3. Characterization

3.1 Characterization of lignin nanoparticles

The particle size analysis of prepared LNP was performed through dynamic light scattering (DLS) Malvern Metasizer nano series – Nano ZS (USA) and transmission electron micrscopy (TEM) (JEOL-1200 EX electron microscope) at accelerating voltage of 80 kV.

3.2Characterization of Bio-PTT/LNP/VGCF hybrid green nanocomposites

3.2.1 Mechanical properties

Tensile properties were determined using universal testing machine (UTM), instruments ltd, UK, as per ASTM-D 638. Tensile test was performed using sample dimension of (165 X 12.7 X3) mm, at a cross-head speed of 10 mm/min and gauge length of 50 mm, Izod impact strength was measured using impacto-meter 6545 (Tinius olsen, Italy) as per ASTM-D 256 with sample dimension of (64.5 X 12.7 X 3) mm with a notch angle of 45^0 and notched depth 2.5 mm.

3.2.2 Heat deflection temperature (HDT)

An HV-2000A-C3, GoTech, (Taiwan) analyzer was used to measure the heat-deflection temperature (HDT) of the bio-PTT, its nanocomposite and hybrid nanocomposites. The HDT measurements were carried out in tensile mode using rectangular specimens of dimension (64.5 X 12.7 X 3) mm with a load of 66 psi and heating rate of 2 ^{0}C / minute.

3.2.3 Thermogravimetric analysis (TGA)

The thermal stability was studied from TGA/DTG thermograms using (TGA Q 50, TA Instruments, USA). Samples of about 10 mg were heated from 50-700^{0}C at a heating rate of 20 ^{0}C / min in nitrogen atmosphere.

3.2.4 Fourier transformation infrared spectroscopy (FTIR)

FTIR spectra of bio-PTT, bio-PTT/LNP, and bio-PTT/LNP/VGCF hybrid nanocomposites were recorded using Nicolet 6700, USA spectrometer. Each spectrum was

obtained by adding 64 consecutive scans with a resolution of 4 cm^{-1} within the range of 500–4500 cm^{-1}.

3.2.5 Water absorption

Water absorption studies of bio-PTT, bio-PTT/1.5 wt.% LNP nanocomposites and bio-PTT/ 1.5 wt.% LNP/7 wt. % VGCF hybrid nanocomposites was performed as per ASTM-D 570. The specimens of size 60 x 60 x 3 mm were initially dried in vacuum oven at 80 °C to remove the moisture for 6 h, cooled in a desiccator and then instantly weighed to the accuracy of 0.001 g. Thereafter, the samples were immersed in distilled water and maintained at 23 ± 2 °C for a 60-day period. During this time, they were removed from the water at 10-day intervals, smoothly wiped with tissue paper to take away over indulgence of water from their surfaces, and weighed to the nearest 0.001 g three times, and returned in water. An average value of the weight measured at each 10-day interval was calculated, the percentage of weight increase due to water absorption (W_f) was calculated to the nearest 0.01% according to Eq. (1):

$$\% W_f = (W_w - W_c) / (W_c) \times 100\% \quad \text{.....(1)}$$

Where, W_f, W_w, and W_c are weight of water absorption, average weight, and initial weight of sample, respectively.

3.2.6 Biodegradation studies

Biodegradation studies of bio-PTT, bio-PTT/ 1.5 wt. % LNP nanocomposites and bio-PTT/ 1.5 wt. % LNP/ 7 wt. %VGCF hybrid nanocomposites was examined by evaluating the weight loss of the nanocomposites over time in soil. Specimens of dimensions (50 mm × 30 mm × 1 mm) were weighed and enclosed in boxes containing alluvial-type soil. Soil was maintained at approximately 35% moisture by weight, and the samples were buried at a depth of 12–15 cm. The samples were unburied after 20 days, washed in distilled water, dried in a vacuum oven at

50 ± 2 ^{0}C for 3 days, and equilibrated in desiccators for at least 1 day. The samples were then weighed before being returned to the soil.

3.2.7 Scanning electron microscopy (SEM)

The morphologies of bio-PTT hybrid nanocomposites after being subjected to biodegradation test were examined employing SEM (EVO MA 15, Carl zeiss SMT, Germany). The samples were Au/Pd sputtered (50 nm) and dried for 30 minute at 70 ^{0}C in vacuum prior to study.

4. RESULT AND DISCUSSIONS

4.1 Dynamic light scattering (DLS) analysis: Particle size determination of LNP

Figure 1 (a) shows the particle size distribution curve as a function of percentage of total particle and particle diameter of LNP. The particle size diameter such as D_{10} (10% of total particle lies below this diameter) to D_{90} (90% of total particle lies below this diameter) and D_{avg} (average diameter of particle) of LNP extracted from DLS spectra is shown in Figure 1(b) and the corresponding data is given in Table 2. As evident from Table 2, the average diameter of particle of LNP is about 181 nm. Figure 1 (a) shows that 60% of total particle lies below of 250 nm range. In fact, the dispersion of the LNP powder to its primary particle size does not happen completely because the attractive force between dry particles is high due to intermolecular H-bonding between the particles[22].

Figure 1. (a) **Particle size distribution for LNP**

Figure 1. **(b) DLS Spectra for LNP**

Table 2. Characteristics particle size of LNP

Furthermore, comparing the particle size of as received lignin and synthesized LNP (Figure 1 a-b), it is observed that in the both cases the average particle diameter is significantly

reduced from 1-200 μm to 1-250 nm. From these results it is also confirmed that applying acid precipitation technique it is possible to obtain nanosized lignin particles.

4.3 Transmission electron microscopy (TEM) of LNP

Typical TEM images of LNP are represented in Figure 2(a-b). TEM image of these LNP confirm that nano-sized precipitates were formed suggesting that LNP may consist of small lignin cluster forming aggregate like structure due to hydrogen bonding between the particles. Hence, the sample was sonicated for 10 minute to break-up particle aggregates and to re-disperse the particles. It was observed that not all particle aggregates broke-up completely. Our assumption is that upon acid precipitation from ethylene glycol solution, the planar phenol groups present in lignin are stacked in layer and are densely packed within the NP [23]. The TEM images show the smallest particle size to about of 5.79 nm and bigger particle size to about of 117.72 nm. This confirms the size of LNP is consistent with those from particle size determined by the DLS. Typically, the calculated size is expressed as the diameter of a sphere that has the same projected area as the projected image of the particle.

Figure 2. TEM micrograph for LNP

4.4 Mechanical properties.

4.4.2 Mechanical properties of bio-PTT/LNP/VGCF Hybrid Green Nanocomposites

The mechanical properties of bio-PTT, bio-PTT/1.5wt.%LNP nanocomposites and bio-PTT/1.5wt.%LNP/VGCF hybrid nanocomposites at variable concentration of VGCF (3, 5, 7, & 10 wt. %) are depicted in Table 3. It is evident that the tensile strength and modulus of bio-PTT increased by 14.86 %, and 8.26 % with the incorporation of 1.5 wt.% of LNP, respectively, which possibly indicates the reinforcing effect of the filler within the matrix polymer. A similar increase in flexural strength, modulus and impact strength to the tune of 14.89%, 10.24% and

30.93% was observed. Additionally, with the incorporation of VGCF within the nanocomposites matrix, results in improved mechanical performance. The hybrid nanocomposites at 7 wt.% VGCF exhibited optimum strength and modulus as compared with the virgin matrix. This behavior is primarily due to improved interaction between VGCF and bio-PTT at the interface. Also it is assumed that during melt mixing VGCF breaks down and gets dispersed within the matrix uniformly while destroying the aggregates of LNP. Hence the synergistic effect of LNP and VGCF contributes to an increase in modulus.[24,25]

Furthermore, the bio-PTT/1.5 wt.% LNP/7 wt.% VGCF hybrid nanocomposite show higher. The flexural strength and modulus increased by 21.90% and 29.54%, respectively of 7 wt.% VGCF content hybrid nanocomposite as compared with bio-PTT. This confirm that, VGCF are distributed uniformly within bio-PTT matrix and the force transfer from bio-PTT to VGCF linearly increased with the VGCF content up to 10 wt. %.

Table 3. Mechanical properties of Bio-PTT/LNP/VGCF hybrid green nanocomposites

The impact strength of bio-PTT/LNP/VGCF hybrid nanocomposites was also found to increase as compared with the bio-PTT/LNP nanocomposite as well as the bio-PTT matrix. Impact strength of 38.52J/m was observed in bio-PTT/1.5wt.%LNP nanocomposite, which 12.07% higher in case of bio-PTT/1.5 wt. % LNP/7 wt. %VGCF hybrid nanocmoposite. Hence, impact strength of nanocomposites as well as hybrid nanocomposites was found to increased as compared to bio-PTT (29.42J/m). This improvement in the impact strength may be attributed to the uniform distribution of LNP and VGCF within the bio-PTT matrix. No further improvement in impact strength has been noticed at higher VGCF content (i.e. 10 wt. %) hybrid nanocomposite. This may be due to the debonding of VGCF and mobility in the bio-PTT matrix make possible the energy decapitation, which causes the toughening of the composites. [26, 27]

With the increasing of VGCF beyond 7 wt.%, the strain at break is decreased dramatically. This is assumed that the formation of VGCF network restricts the mobility of bio-PTT chain, leading to brittle response.

4.5 Heat deflection temperature (HDT)

The HDT value of bio-PTT, bio-PTT/1.5 wt. % LNP, and various concentrations i.e. 3, 5, 7 and 10 wt. % of VGCF content in bio-PTT/1.5 wt. % LNP hybrid nanocomposites has been represented in Figure 3. It is observed that the HDT of bio-PTT increases with the incorporation of LNP particles, suggesting that LNP particles have good effect on improving the thermal resistance of bio-PTT. The HDT value of bio-PTT/1.5wt.% LNP increases to the tune of 117.7% as compared to the bio-PTT matrix. Furthermore, incorporation of VGCF with bio-PTT/1.5 wt. % LNP nanocomposites shows that improved the HDT of bio-PTT matrix. The HDT values were observed to increased by 209.8%, 214.4%, 231.5% and 252.5% for bio-PTT/1.5 wt.% LNP/3 wt. %VGCF, bio-PTT/1.5 wt. %LNP/5 wt. %VGCF, bio-PTT/1.5 wt. % LNP/7 wt. %VGCF and bio-PTT/1.5 wt.% LNP/10 wt. %VGCF hybrid nanocomposites , respectively as compared with bio-PTT matrix. The highest HDT value was obtained in 10 wt. % VGCF content in bio-PTT/1.5 wt. %LNP hybrid nanocomposites. This observed enhancement of HDT may be attributed to the better dispersion of VGCF within bio-PTT matrix. It is very difficult to achieve high HDT enhancement without a strong interaction among the fillers and polymer matrix. These results suggest that the improvement in HDT in bio-PTT originates from the better reinforcement by the dispersed phase of LNP and VGCF their intercalation within the bio-PTT matrix.[28]

Figure 3. HDT value for bio-PTT, bio-PTT/LNP nanocomposites and bio-PTT/LNP/VGCF hybrid nanocomposites

4.6 Thermo gravimetric analysis (TGA)

The weight loss and derivative weight loss of bio-PTT and its hybrid nanocomposites are represented in Figure 4. TGA results revealed that the initial degradation temperature (T_{id}), the temperature at 50% weight loss ($T_{50\%\ wt.\ loss}$) and final degradation temperature (T_{fd}) of bio-PTT and its hybrid nanocomposite (enumerated in Table 4) were found to be increased with the incorporation of VGCF. Bio-PTT exhibited an initial degradation temperature (T_{id}) of 325 ^{0}C and final degradation temperature (T_{fd}) of 427 ^{0}C. The degradation process was mainly caused by degradation of the polymer chain implying an end group initiation mechanism affected by the molecular weight of bio-PTT. This effect is a result of relatively good thermal stability of hydroxyl terminal groups in bio-PTT which initiate thermal degradation of bio-PTT.[29]

Figure 4: TGA curve for weight loss and derivative weight loss of bio-PTT and its hybrid nanocomposites

The temperature of the maximum weight loss is shifted towards higher side in nanocomposites. The obtained results show that the thermal stability of bio-PTT increases with the addition of LNP. Incorporation of LNP increases T_{id} of bio-PTT matrix from 325 ^{0}C to 337 ^{0}C and T_{fd} from 427 ^{0}C to 447 ^{0}C. The improvement in the thermal stability of nanocomposites can be attributed to the thermal shielding effect of LNP. The small molecules generated during the thermal decomposition process cannot permeate LNP slow down the release rate of decomposed by products thereby enhance the thermal stability of the nanocomposites.[30]

Table 4. TGA degradation temperature results of bio-PTT and its hybrid nanocomposites

On the other hand, VGCF loaded bio-PTT/LNP hybrid nanocomposites found to have unique thermal stability. The TGA data display that the T_{id} and T_{fd} of hybrid nanocomposites

were found to be higher side than that of bio-PTT/LNP nanocomposite as well as bio-PTT matrix. Incorporation of VGCF increases T_{id} of bio-PTT hybrid nanocomposites from 337 ^{0}C to 344 ^{0}C and T_{fd} from 447 ^{0}C to 542 ^{0}C. The hybrid nanocomposites containing 7 wt. % VGCF is exhibits the highest T_{id} and T_{fd} values, which may be due to the strong interaction of LNP and VGCF which restrict thermal motion of the bio-PTT molecules. In other words, the presences of VGCF within the bio-PTT/LNP greatly restrain their thermal degradation at high temperature.[31]

4.7 FTIR analysis of bio-PTT and its nanocomposites

The FTIR spectra of bio-PTT, LNP, VGCF, bio-PTT/1.5 wt.% LNP nanocomposites and bio-PTT/1.5 wt.% LNP/7 wt.% VGCF hybrid nanocomposites are shown in Figure 5. The possible reaction scheme between LNP and bio-PTT is represented in Figure 6. The characteristics peak for LNP at 1586 cm^{-1} which appears due to the C-H deforming vibrations in ethylene glycol present in LNP. LNP exhibited peaks characteristics of polar groups, such as alcohols (3383, 1217 and 1028 cm^{-1} bands).[32] Furthermore, the characteristics peaks for VGCF observed corresponding to the hydroxyl groups (–O–H stretching vibration) between 3365 and 2242 and 3374 cm^{-1}. In addition, many bands corresponding to nonaromatic vibrations and aromatic C–H signals appeared. Among these bands there are: (1) the aromatic C–H stretching signal of arenes (several bands at around 3020 cm^{-1}), (2) different small bands at about 1493 and 1443 appearing as shoulders on the right of the band at 1586 cm corresponding to an aromatic C=C ring stretch, these bands may be attributed to the asymmetrical bending vibration of methyl groups that overlap with the scissoring vibration of methylene groups, (3) the –O–H bending (in plane) between 1352 and 1430 cm^{-1}, (4) the C–O–C and C–O stretch vibrations at 1217 cm^{-1}, (5) the signal corresponding to the out of plane C–H vibration at about 777 cm^{-1} that overlaps with the signal corresponding to the –O–H bend (out of plane).[33]

Moreover, the characteristics peaks for bio-PTT at 2600-3200, 1700-1750, and 500-1600 cm^{-1} appeared in FTIR spectra. Two extra shoulder characteristics of ester carboxyl groups were observed at 1730 cm^{-1} in the LNP incorporated bio-PTT nanocomposites. At 1720 cm^{-1} and 3374 cm^{-1} appeared peak assigned to carbonyl and aliphatic hydroxyle group, respectively in the bi-PTT/LNP nanocomposite due to the LNP. The shoulder represents free acid in the bio-PTT nanocomposites and thus indicated the successful hydrogen bonding between LNP and bio-PTT matrix.[34]

In the bio-PTT/LNP/VGCF hybrid nanocomposites, the peak allocated to the O-H stretching vibration at 3200-3400 cm^{-1} intensified due to contributions from the –OH group of LNP and VGCF. The FTIR spectrum of the bio-PTT/LNP/VGCF hybrid nanocomposites exposed a peak at 1708, 2862, and 2934cm^{-1} that was not present in the FTIR spectrum of the bio-PTT/LNP nanocomposites. This peak was allocated to the ester carbonyl stretching vibration and C-H stretching vibration of the polymer. These spectral data indicates the creation of split and cross-linked macromolecules in bio-PTT/LNP/VGCF by covalent reaction of the VGCF group in bio-PTT/LNP nanocomposites with the hydroxyl groups of LNP and VGCF.[35]

Figure 5. FTIR spectra for bio-PTT and its nanocmopsoites

Figure 6. Possible reaction scheme between LNP and bio-PTT

4.8 Water absorption of bio-PTT, its nanocomposites and hybrid nanocomposties

The water absorption behavior of bio-PTT, its nanocomposites and hybrid nanocomposites is depicted in Figure 7. It is evident that the percentage of water absorption increases in the entire sample with time. Bio-PTT matrix showed lowest water absorption with the nanocomposites sample exhibiting maximum tendency to absorb water within the investigated experimental range. Bio-PTT/1.5 wt. % LNP/7 wt. % VGCF depicted a moderate

water absorption tendency using in between the matrix polymer and high moisture absorption tendency of LNP which results in more water uptake in to the nanocomposites. The presence of hydrophobic VGCF might have contributes in lesser tendency of water absorption. [36]

Figure 7. Percent weight gain due to the absorption of water for bio-PTT, bio-PTT/LNP, and bio-PTT/LNP/VGCF nanocomposites.

4.9 Biodegradation studies of bio-PTT, its nanocomposites and hybrid nanocomposites

SEM microgarphs of bio-PTT, bio-PTT/1.5wt.%LNP nanocomposites and bio-PTT/1.5wt.%LNP/7wt.%VGCF hybrid nanocomposite samples buried under soil medium taken after 60 and 120 days, respectively are shown in Figure 8. Bio-PTT/1.5 wt. % LNP/7 wt % VGCF hybrid nanocomposites (Fig. 8 h and i) exhibited larger and deeper pits that appeared to be more randomly distributed than those in the bio-PTT/1.5 wt. % LNP nanocomposites (Fig. 8 e and f). The micrographs also indicated that biodegradation of the VGCF phase in bio-PTT/1.5 wt % LNP increased with time, confirming the results presented in Figure 9. Following 60 days, the interference of the bio-PTT matrix became more noticeable. This degradation was confirmed by increasing weight loss of the bio-PTT matrix as a function of incubation time, which reached almost 15% after only 120 days. The most likely cause of this weight loss was biodegradation. The SEM images suggest that the bio-PTT/1.5 wt. %LNP/7 wt. % VGCF hybrid nanocomposites showed more degradation tendency than bio-PTT. Moreover, at 60 and 120 days, larger pores were visible in the bio-PTT/1.5wt.%LNP/7wt.%VGCF hybrid nanocomposite (Fig. 8 h and i), representing upper stage of degradation.

Figure 9 shows the percent weight change as a function of time for bio-PTT, bio-PTT/1.5wt.%LNP nanocomposites and bio-PTT/1.5wt.%LNP/7wt.%VGCF hybrid nanocomposites buried in the soil compost. The rate of weight loss of the bio-

PTT/1.5wt.%LNP/7wt.%VGCF hybrid nanocomposites was also accelerated relative to that of bio-PTT, beyond 25% after 120 days. These results demonstrate that the addition of VGCF to the bio-PTT/1.5 wt. % LNP nanocomposites improved the biodegradability of the hybrid nanocomposite.[37] The degree of weight loss was increased due to LNP and VGCF content in bio-PTT hybrid nanocomposites.

Figure 8. SEM morphology of bio-PTT, bio-PTT/1.5 wt % LNP and bio-PTT/1.5 % LNP/7wt % VGCF hybrid nanocomposites as a function of incubation time in soil.

Figure 9. Weight loss percentages of bio-PTT, bio-PTT/LNP, and bio-PTT/LNP/VGCF hybrid nanocomposites as a function of incubation time in soil

5. Conclusion

The biodegradability and mechanical properties of bio-PTT/LNP/VGCF hybrid nanocomposites were examined. Mechanical findings, revealed 19.90 %, 12.19 % and 46.73 % improvement in tensile strength, tensile modulus and impact strength, respectively with the incorporation of 7 wt. % of VGCF within the bio-PTT/1.5 wt. %LNP nanocomposite. The TGA results revealed that the thermal stability of bio-PTT and its hybrid nanocomposites improved and heat deflection temperature increased three fold times of bio-PTT upon reinforcement with VGCF. FTIR analysis revealed the formation of interaction between the aliphatic –OH groups in LNP and VGCF with the carbonyl group of bio-PTT matrix. Although, the water resistance of bio-PTT/LNP/VGCF hybrid nanocomposites was higher than that of bio-PTT/LNP nanocomposites. The biodegradation rate of bio-PTT/LNP/VGCF hybrid nanocomposites was lower than that of bio-PTT/LNP nanocomposites, but still higher than that of bio-PTT, when incubated in soil. After 120 days, the bio-PTT/LNP/VGCF hybrid nanocomposites showed more than 60% weight loss in soil medium. Thus, the bio-PTT/LNP/VGCF hybrid nanocomposites

exhibited good mechanical and thermal properties, and biodegradation characteristics which can be suitably used for various end-use applications.

References

1. L. S. Schadler, L. C. Brinson, and W. G. Sawyer, J. Min. Met. Mat. Soc. 2007, 59, 53.
2. A.K. Mohanty, M. Misra, L.T. Drzal, S.E. Selke, B.R. Harte, and G. Hinrichsen, CRC Press: Boca Raton, FL, USA, 2005.
3. K. Oksman, A.P. Mathew, D. Bondeson, and I. Kvien, Compos. Sci. Technol. 2006, 66, 2776
4. 4. M. Darder, P. Aranda, and E.Ruiz-Hitzky, Adv. Mat. 2007, 19, 1309
5. G.G. Tibbetts, M.L. Lake, K.L. Strong, and B.P. Rice. Compos Sci Technol. 2007, 67, 1709
6. M.H. Al-Saleh, and U. Sundararaj, In: Society of plastics engineers annual technical conference – ANTEC. Milwaukee, WI, USA, 2008, 34
7. M.H. Al-Saleh, and U. Sundararaj. Carbon. 2009, 47, 2
8. S. W. Kim, W. H. Jo, M. S. Lee, M. B. Ko, and J. Y. Jho, Polym. J. 2002, 34 (3), 103.
9. I. Szleifer, and R. Yerushalmi-Rozen, Polymer, 2005**,** 46, 7803.
10. H. R. Dennis, D. L. Hunter, D. Chang, S. Kim, J. W. Cho, and D. R. Paul, Plast. Eng. 2001, 1, 56.
11. W. Kunyan, C. Yanmo, and Z. Yu, Polymer. 2008, 49, 3301.
12. J. Zhang. J. Appl. Polym. Sci. 2004, 91, 1657
13. W.J. Liu, A.K. Mohanty, L.T. Drzal, M. Misra, J.V. Kurian, R.W. Miller, and N. Strickland, Ind. Eng. Chem. Res., 2005, 44, 857
14. A.K. Gupta, S. Mohanty, S.K. Nayak, *Materials Focus.* 2014, 3, 144

15. C. Frangville, M. Rutkevicius, A.P. Richter, O.D. Velev, S.D. Stoyanov, and V.N. Paunov, ChemPhysChem. 2012, 13, 4235

16. P. Gonugunta, V. Singaravelu, K.M. Amar, and M. Manjusri, *World Journal of Nano Science and Engineering,* 2012, 2, 148

17. K. C. Chang, K. Matsugi, G. Sasaki and O. Yanagisawa. J. Japan Inst. Metals. 2005, 69, 983

18. K. C. Chang, K. Matsugi, G. Sasaki and O. Yanagisawa: JSME Int. J. 2005, 48, 205

19. E. Sato, T. Takahashi, T. Natsume and K. Koyama: Tanso. 2003,109, 159

20. Show Denko Co., Ltd.: Material Safety Data Sheet 2007.

21. M. Endo, Y. A. Kim, T. Hayashi, K. Nishimura, K. Miyashita and M. S. Dresselhaus. Carbon. 2001, 39,1287

22. A.F. Rawle, Powder Technology, 2007,174, 6.

23. A.Rawle, Advances in color science and technology, 2002, 5, 12.

24. K. Lozano, et al. In: Powder materials: current research and industrial practice (as held at the TMS Fall Meeting), Ohio: Cincinnati; 1999.

25. J.S. Hong, H. Nam Kung, K.H. Ahn, et al. Polymer. 2006, 47, 3967

26. T.H. Zhou, W.H. Ruan, M.Z. Rong, M.Q. Zhang, and Y.L. Mai, Adv. Mater. 2007, 19(18), 2667.

27. D. Shah, P. Maiti, D.D. Jiang, C.A. Batt, E.P. Giannelis, Adv. Mater. 2005,17(5),525.

28. J.M. Ting, and M.L. Lake. J Mater Res. 1995, 10(2), 247

29. J. Liu, S. G. Bian, M. Xiao, S. J. Wang, and Y. Z. Meng, Chinese Chemical Letters. 2009, 20, 487

30. H. J. Yoo, Y. C. Jung, and J. W. Cho, Journal of Polymer Science Part B: Polymer Physics. 2008, 46, 900

31. M. Avella, M. E. Errico, and E. Martuscelli, Nanoletters. 2001, 1, 213

32. X. Pan, J.F. Kadla, K. Ehara, N. Gilkes, J.N. Saddler, and J. Agric. Food Chem. 2006, 54, 5806.

33. Endo M et al. Carbon. 2001 ,39, 1287

34. S. Kubo, and J. F. Kadla, Biomacromolecules. 2005, 6 (5), 2815.

35. Z.Tang , D. Sun , D. Yang , B. Guo , L. Zhang , and D. Jia, Composites Science and Technology. 2013, 75, 15.

36. C. S. Wu, Journal of Applied Polymer Science. 2011, 121, 427

37. L. S. Nair, and C. T. Laurencin, Progress in Polymer Science. 2007, 32, 762

Figure caption

Figure 1. (a) Particle size distribution for LNP

Figure 1. (b) DLS Spectra for LNP

Figure 2. TEM micrograph for LNP

Figure 3: HDT value curve of bio-PTT and its hybrid nanocmposites

Figure 4: TGA curve for weight loss and derivative weight of bio-PTT and its hybrid nanocomposites

Figure 5. FTIR spectra for bio-PTT and its hybrid nanocmopsoites

Figure 6. Possible reaction scheme between LNP and bio-PTT

Figure 7. Percent weight gain due to the absorption of water for bio-PTT, bio-PTT/1.5 wt. % LNP, and bio-PTT/1.5 wt. % LNP/7 wt. % VGCF hybrid nanocomposites.

Figure 8. SEM morphology of bio-PTT, bio-PTT/1.5 wt %, LNP and bio-PTT/1.5 wt. % LNP/7 wt. % VGCF hybrid nanocomposites as a function of incubation time in soil.

Figure 9. Weight loss percentages of bio-PTT, bio-PTT/1.5 wt. % LNP, and bio-PTT/1.5 wt. % LNP/7 wt. % VGCF hybrid nanocomposites as a function of incubation time in soil.

Table caption

Table 1. Typical properties of Bio-PTT and PTT

Table 2. Characteristics particle size of LNP

Table 3. Mechanical properties of bio-PTT, bio-PTT/1.5 wt. % LNP and bio-PTT/1.5 wt. % /VGCF hybrid green nanocomposites

Table 4. TGA degradation temperature results of bio-PTT and its hybrid nanocomposites

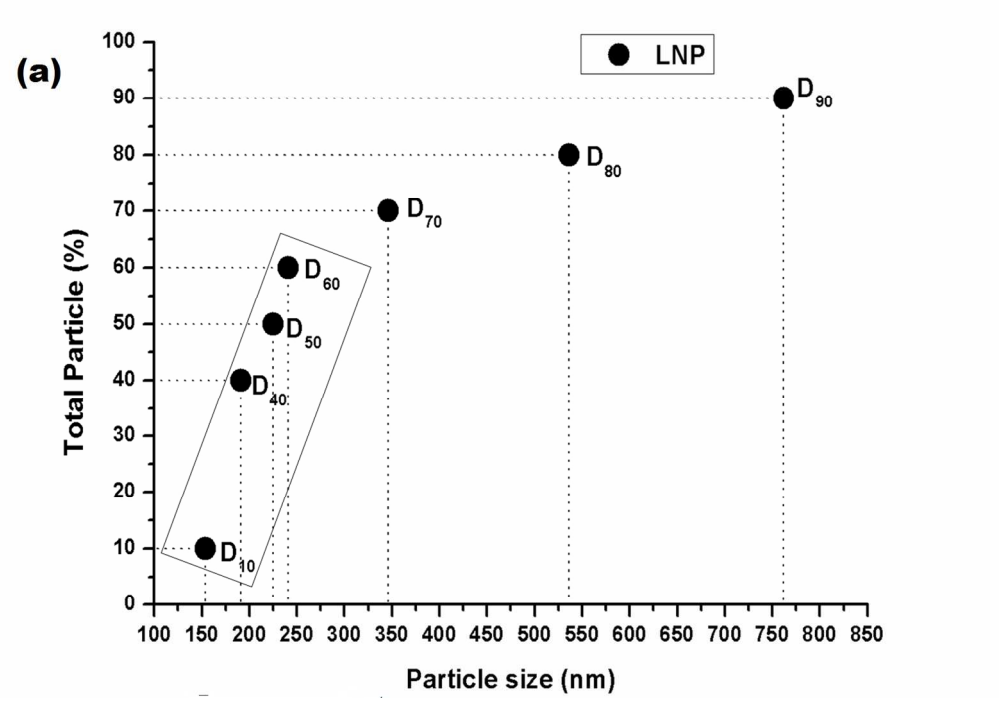

Figure 1. (a) Particle size distribution for LNP
169x118mm (300 x 300 DPI)

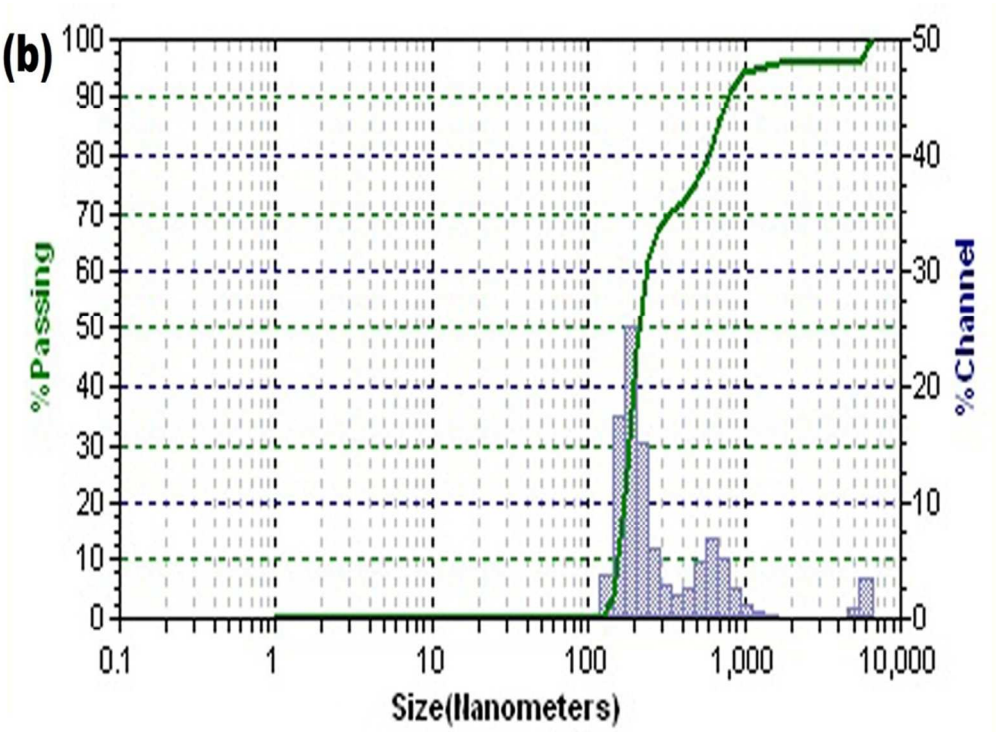

Figure 1. (b) DLS Spectra for LNP
177x129mm (300 x 300 DPI)

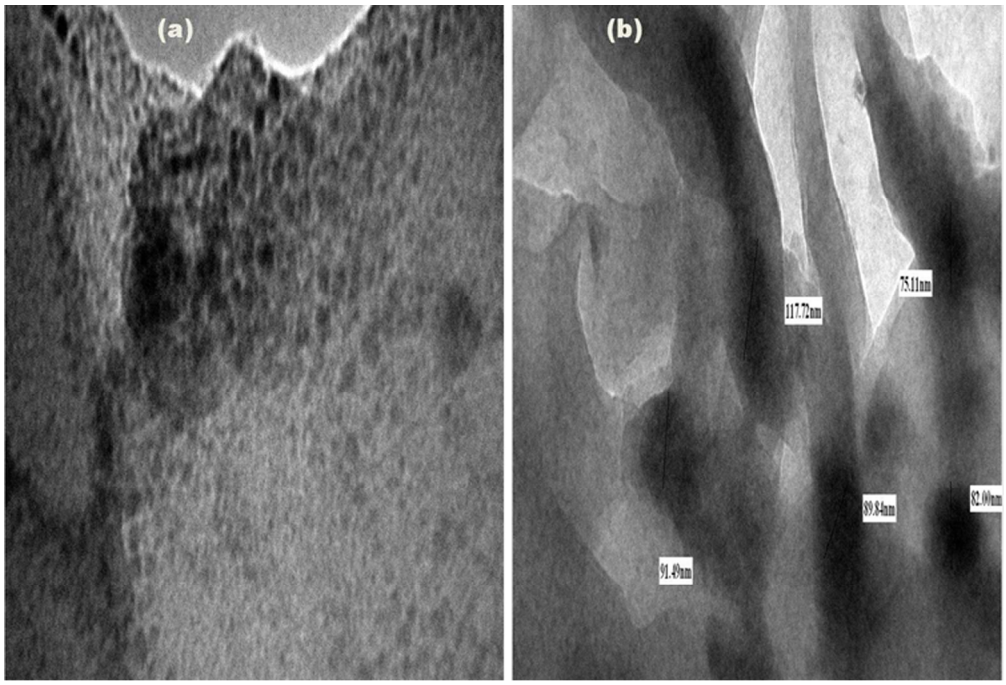

Figure 2. TEM micrograph for LNP
177x119mm (300 x 300 DPI)

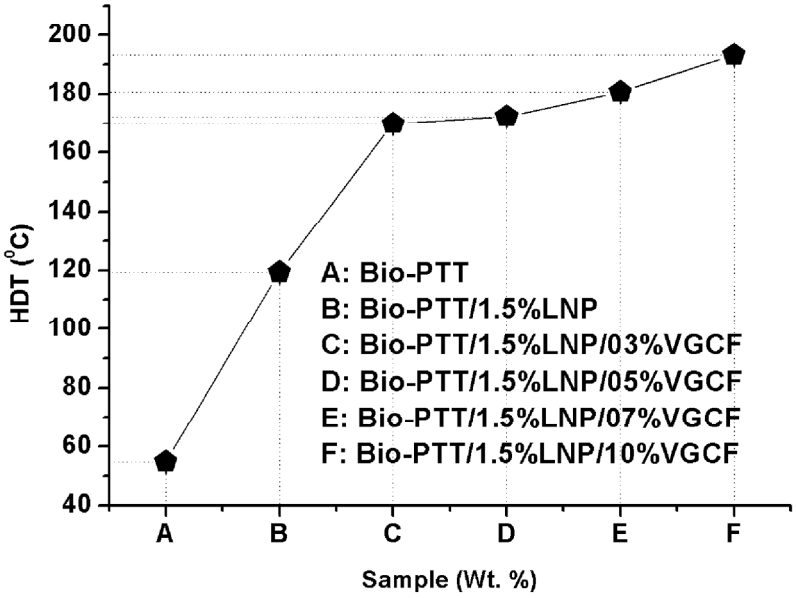

Figure 3: HDT value curve of bio-PTT and its hybrid nanocmposites
177x123mm (300 x 300 DPI)

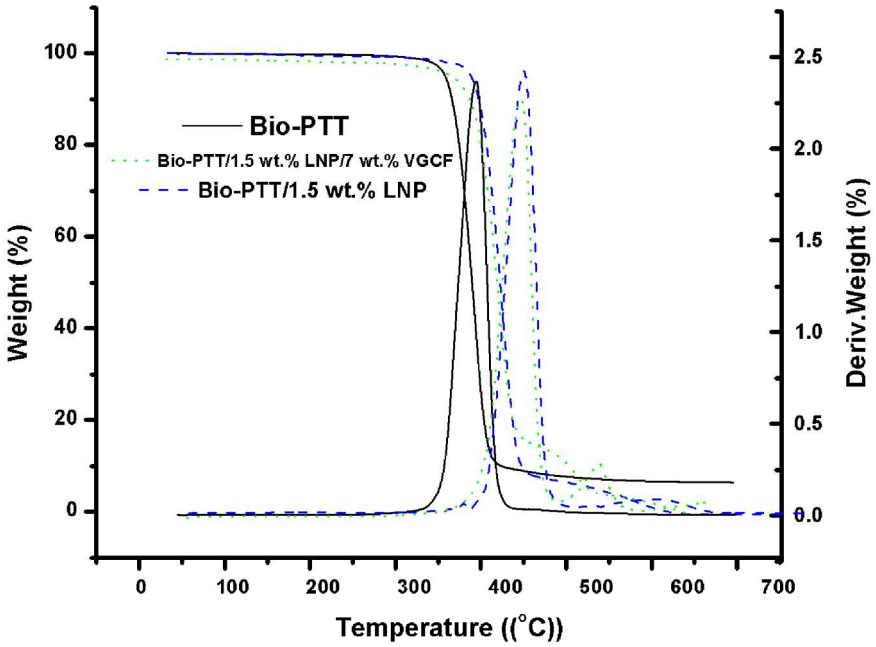

Figure 4: TGA curve for weight loss and derivative weight of bio-PTT and its hybrid nanocomposites
177x136mm (300 x 300 DPI)

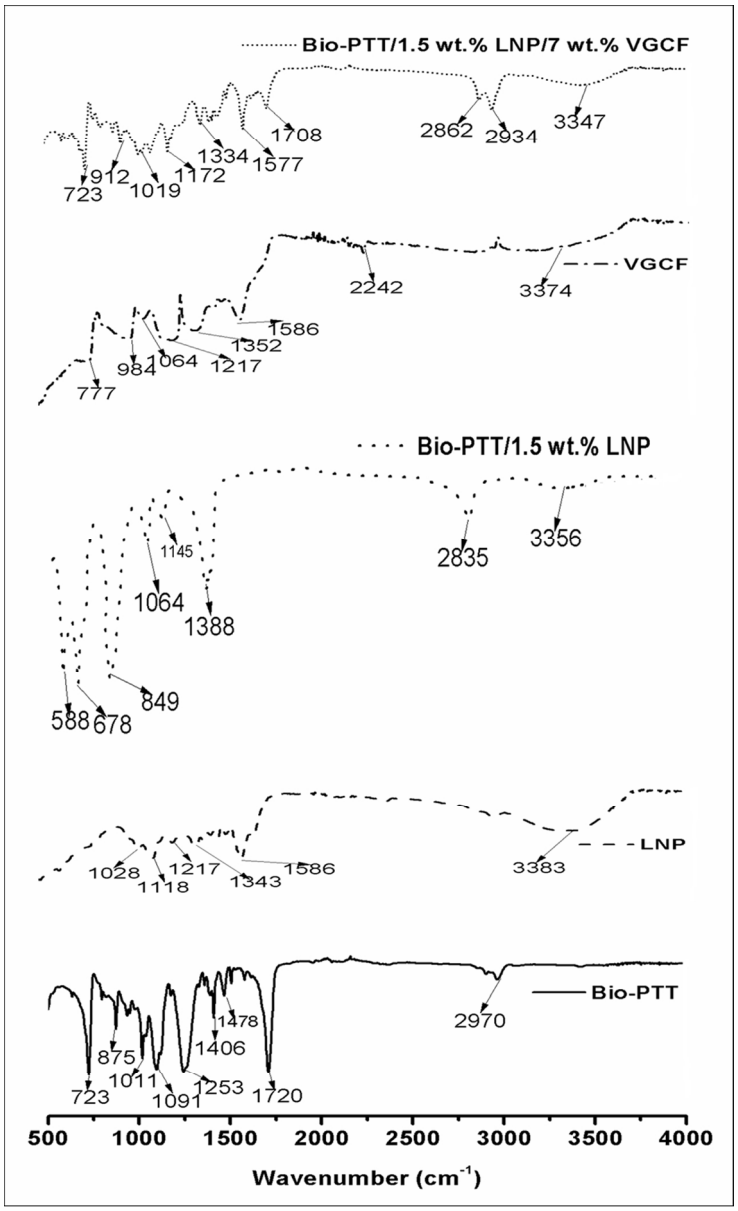

Figure 5. FTIR spectra for bio-PTT and its hybrid nanocmopsoites
107x177mm (300 x 300 DPI)

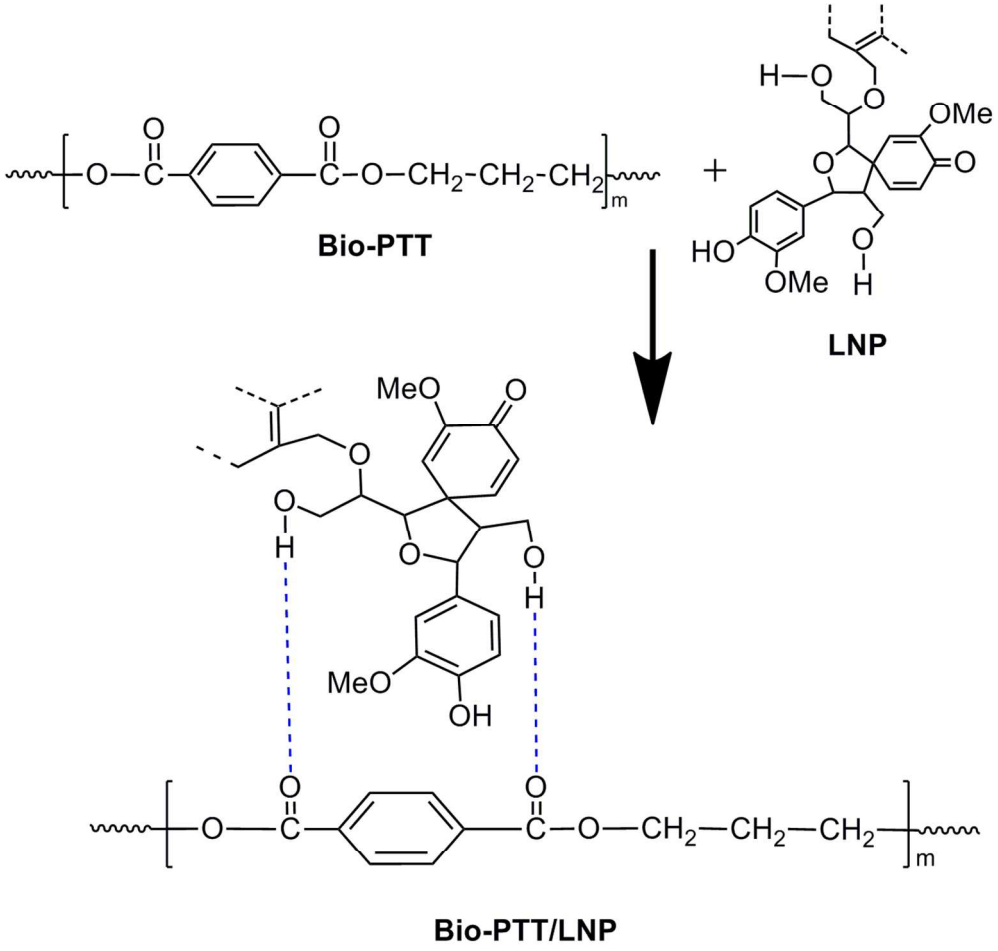

Figure 6. Possible reaction scheme between LNP and bio-PTT
116x111mm (300 x 300 DPI)

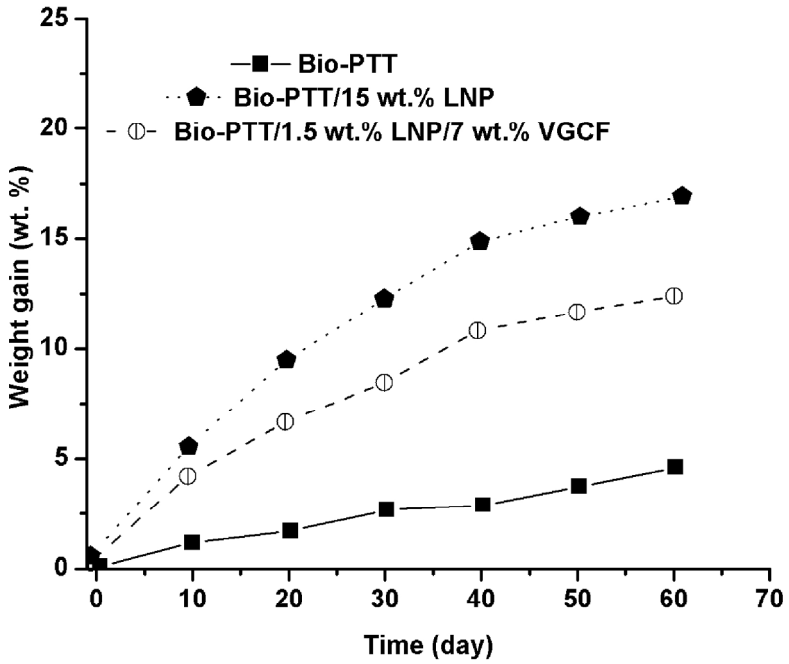

Figure 7. Percent weight gain due to the absorption of water for bio-PTT, bio-PTT/1.5 wt. % LNP, and bio-PTT/1.5 wt. % LNP/7 wt. % VGCF hybrid nanocomposites.
177x136mm (300 x 300 DPI)

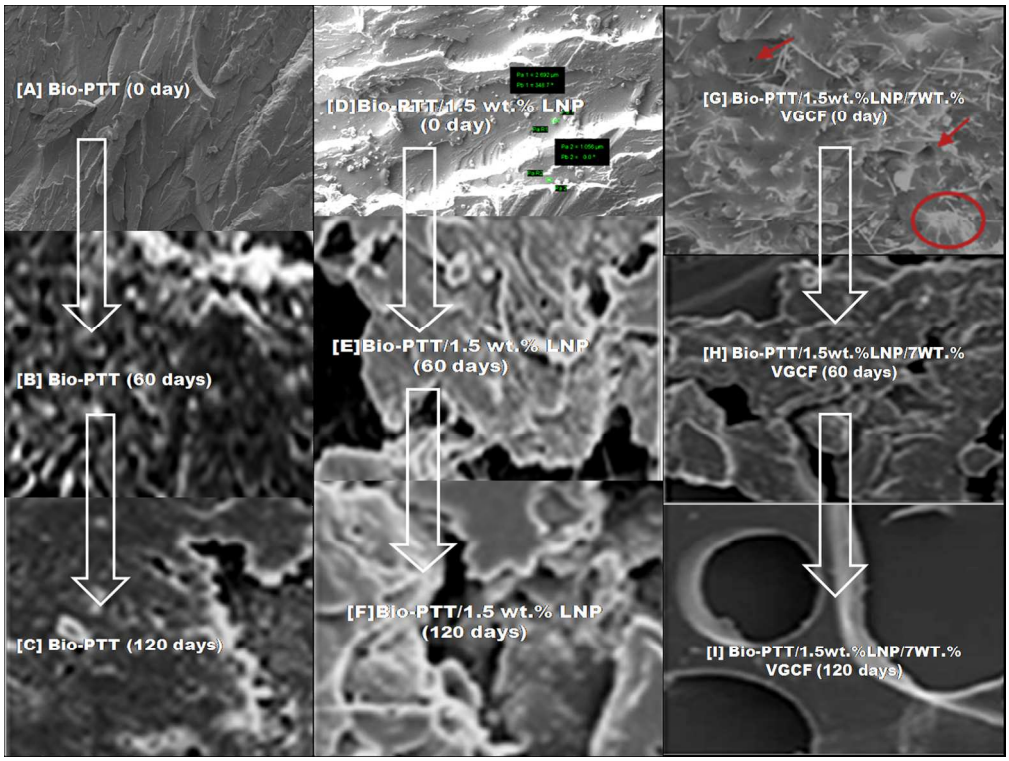

Figure 8. SEM morphology of bio-PTT, bio-PTT/1.5 wt %, LNP and bio-PTT/1.5 wt. % LNP/7 wt. % VGCF hybrid nanocomposites as a function of incubation time in soil.
177x133mm (300 x 300 DPI)

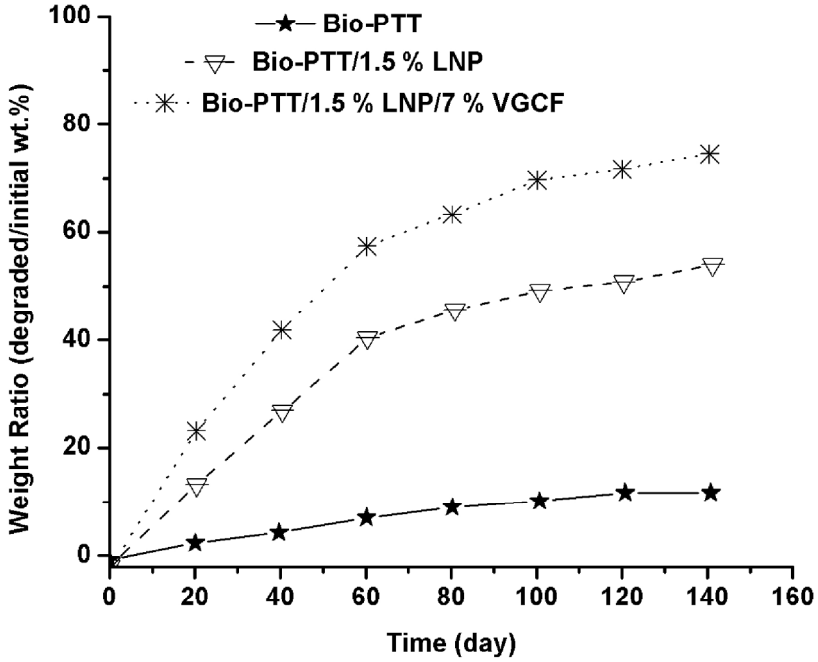

Figure 9. Weight loss percentages of bio-PTT, bio-PTT/1.5 wt. % LNP, and bio-PTT/1.5 wt. % LNP/7 wt. % VGCF hybrid nanocomposites as a function of incubation time in soil.
177x136mm (300 x 300 DPI)

Table 1. Typical properties of Bio-PTT and PTT

Property	Value	
Product description	**Bio-PTT**	**PTT**
Grade	Biomax® PTT 1002: PDO/TPA	CORTERA PTT 200: PDO/DMT
Composition	37% by weight bio-sourced	……
Source of diol	Corn sugar	Chemically derived propylene glycol
Melt flow index (225 ^{0}C/1.16 kg)	19 g/10min	10min12 g/
Density @ 23 ^{0}C	1.33 g/cc	1.47 g/cc
Intrinsic viscosity (IV)	1.02 dl/g	0.85 dl/g
Processing temperature	260 ^{0}C	245 ^{0}C
Melting temperature (T_m)	228 ^{0}C	227 ^{0}C
Glass transition temp. (T_g)	55 ^{0}C	51 ^{0}C
Heat deflection temperature (0.455 MPa)	55 ^{0}C	53 ^{0}C
Tensile strength yield (50 mm/min)	51 MPa	35 MPa
Notched izod impact strength (23 ^{0}C)	30 J/m	18 J/m

Table 2. Characteristics particle size of LNP

Characteristics particle diameter	Size range (nm)
$\mathbf{D_{10}}$	154
$\mathbf{D_{40}}$	191
$\mathbf{D_{50}}$	225
$\mathbf{D_{60}}$	241
$\mathbf{D_{70}}$	346
$\mathbf{D_{80}}$	536
$\mathbf{D_{90}}$	762
$\mathbf{D_{Average}}$	181

Table 3. Mechanical properties of Bio-PTT/LNP/VGCF hybrid green nanocomposites

Sample (Wt. %)	Tensile strength (MPa)	Tensile modulus (MPa)	Flexural strength (MPa)	Flexural modulus (MPa)	Impact strength (j/m)
Bio-PTT (100/0)	51.49 ± 0.5	2057.89 ± 37	76.89 ±0.6	2382.26 ± 21.9	29.42± 1.2
Bio-PTT/LNP (98.5/1.5)	59.16 ± 0.7	2227.21 ± 47	88.25± 1.3	2626.23± 24.3	38.52± 1.8
Bio-PTT/LNP/VGCF (95.5/1.5/3)	52.32± 0.8	2138.61± 59	80.72± 1.4	2787.81± 64	28.99± 0.2
Bio-PTT/LNP/VGCF (93.5/1.5/5)	57.89± 0.3	2272.21± 48	83.91± 1.7	2824.59± 72	34.82± 0.8
Bio-PTT/LNP/VGCF (91.5/1.5/7)	61.74± 0.6	2308.89± 69	93.73± 0.8	3086.18± 63	43.17± 0.6
Bio-PTT/LNP/VGCF (88.5/1.5/10)	61.38± 0.9	2305.64± 57	92.89± 0.9	3164.40± 53	42.92± 0.9

Table 4. TGA degradation temperature results of bio-PTT and its hybrid nanocomposites

Sample (wt. %)	T_{id} (^{0}C)	T_d at 50$_{\%}$ (^{0}C)	T_{fd} (^{0}C)	%Char content
Bio-PTT	325	365	427	9.36
Bio-PTT/1.5% LNP	337	386	447	7.62
Bio-PTT/LNP/7%VGCF	344	397	542	2.89